Applied and Computational Mathematics
2025, Vol. 14, No. 3, pp. 164-182
https://doi.org/10.11648/j.acm.20251403.14

Research Article

Mathematical Modelling and Analysis of the Non-Linear Multi-Layer Amperometric Biosensor with Degradation of Concentrations Derived by Analytical Expressions in Chemical Sciences

Ranjani Kesavan, Swaminathan Rajagopal, Karpagavalli Ramasamy*

PG & Research Department of Mathematics, Vidhyaa Giri College of Arts and Science (Affiliated to Alagappa University), Puduvayal, India

Abstract

A mathematical model has been developed to assess the multilayer heterogeneous biocatalytic system. A nonlinear system of the mathematical model's analytical expressions for the non-steady state conditions obtained by the new homotopy perturbation method (NHPM) has been computed. In the mathematical model, there are three scenarios: When the substrate degradation diffuses out of the biosensor, when the product diffuses for the biosensor and when both the substrate and product degradation diffuse for the biosensor. Profiles of how the substrate and product degradation rates do not affect the biosensor response have been created in three situations. The third situation is solved by the Akbari-Ganji method (AGM), which describes not effect of degradation rates' impact on the biosensor response. Furthermore, the numerical simulations of the problem are presented using MATLAB. These numerical results are compared with analytical results, and a good agreement is obtained. A graphical procedure is carried out for the degradation rates of species, kinetic parameters and current for steady and non-steady state conditions.

Keywords

Biosensor, Degradation Rates of Concentration, Mathematical Modeling, New Homotopy Perturbation Method, Akbari-Ganji Method

1. Introduction

Biosensors have a wide range of uses in both industry and medicine. Biosensor response of Amperometric, Potentiometric and its applications [1, 2], the numerical algorithm presented [3-6]. In multiple technical and scientific fields, linear and non-linear phenomena are fundamentally significant. The majority of models of real-world issues remain highly challenging to resolve. It is inappropriate to consider the mathematical modelling of a multilayer heterogeneous analytical system due to the accumulation of independent models defined in corresponding layers. The complete multilayer biosensor must be treated as a single, integrated system in mathematical analysis. The proposed mathematical modelling

*Corresponding author: sgkarpa@gmail.com (Karpagavalli Ramasamy)

Received: 14 May 2025; **Accepted:** 29 May 2025; **Published:** 18 June 2025

of the biosensor action can define a range of biosensor parameters and their weights in response formation.

Many electrochemical biosensors have at least two layers: an outer protection membrane and an enzyme layer. Several mechanisms (enzymatic reaction, diffusion, degradation) can occur in some or all layers to produce the biosensor response; nevertheless, these processes interact in specific nontrivial ways. Hence, rather than attempting to total the results of various models described in the appropriate levels, mathematical and numerical modelling of a multilayer biosensor must treat all layers as one integrated system [3-6].

In actual situations, a variety of internal and external elements have an impact on the biosensor's reaction. A substrate (a) can be consumed (or degraded) by unrelated enzymes, microbes, spontaneous decomposition, or other side reactions after it has been transformed into a product (b) in the enzymatic layer. Similar causes can cause the degradation of product P as well [7].

Tadas Meskauskas proposed a numerical electrochemical biosensor model without including substrate and product degradation components Different layers contain enzymatic reaction, diffusion, and degradation of substrate and product in such layers [8]. These layers produce the biosensor response. The biosensor response and numerical algorithm have been reported [8]. Enzymatic reactions can degrade a substrate after transforming it into a product in the enzyme layer. Similar causes can cause the degradation of the product as well. Latterly, T Meskauskas explained numerical simulations for degradation concentrations [9]. This work deals with a mathematical model that accounts for substrate and product degradation (with different degradation rates) [9]. The approximate analytical solution was derived using the new homotopy perturbation method (NHPM). This technique is the most powerful and advantageous for linear and non-linear conditions. A small parameter is assumed when using the perturbation approach.

The primary purpose of this article is to study the analytical expressions corresponding to the non-steady-state concentration of Substrate, Product, Current, and steady-state Current potential curves derived using the new homotopy perturbation method (NHPM). There are three limiting cases in the mathematical model: when the substrate diffuses for the biosensor when the product degradation diffuses out of the biosensor, and when both the substrate and product degradation diffuse for the biosensor is obtained. Three scenarios have led to the creation of profiles showing how the substrate and product degradation rates have no effect on the biosensor response. The Akbari-Ganji method (AGM) resolves the third scenario by degradation rates that do not affect the biosensor's response.

2. Mathematical Formulation of the Problem

The rate of the substrate (a) and the product (b) with degradation is expressed by [8, 9].

$$a \xrightarrow{Enzyme} b \tag{1}$$

$$b \xrightarrow{electrode} \text{c +/- } n_e \; e^{-}(electrons) \tag{2}$$

The scheme of representation of electrochemical biosensor is presented in Figure 1. The system of nonlinear reaction-diffusion equations is given as follows (t > 0)

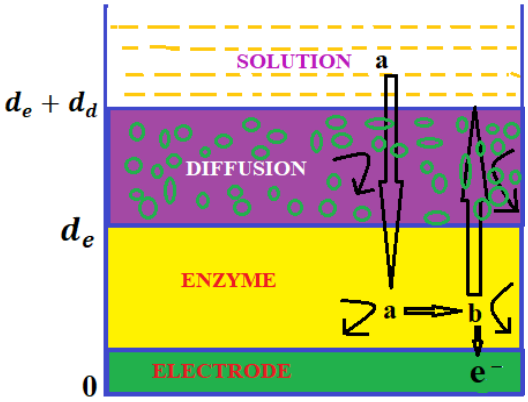

Figure 1. *The electrochemical biosensor schemes.*

For enzyme layer

$$\frac{\partial a_e(x,t)}{\partial t} = D_{a_e}\frac{\partial^2 a_e(x,t)}{\partial x^2} - E_1 a_e - \frac{V_{max} a_e}{K_M + a_e} \tag{3}$$

$$\frac{\partial b_e(x,t)}{\partial t} = D_{b_e}\frac{\partial^2 b_e(x,t)}{\partial x^2} - E_2 b_e - \frac{V_{max} a_e}{K_M + a_e} \quad x \in (0, d_e) \tag{4}$$

For diffusion layer

$$\frac{\partial a_d(x,t)}{\partial t} = D_{a_d}\frac{\partial^2 a_d(x,t)}{\partial x^2} - E_1 a_d \tag{5}$$

$$\frac{\partial b_d(x,t)}{\partial t} = D_{b_d}\frac{\partial^2 b_d(x,t)}{\partial x^2} - E_2 b_d \quad x \in (d_e, d_e + d_d) \tag{6}$$

Where a_e, a_d and b_e, b_d are the substrate and product of enzyme and diffusion layer. D_{a_e}, D_{a_d} and D_{b_e}, D_{b_d} are diffusion coefficient of this layers, V_{max} the rate of the reaction, K_M the Michalis Menten kinetics, E_1 and E_2 are reaction rate of degradation, d_e, d_d are the relative thickness.

The initial and boundary conditions are

For enzyme

$$t = 0, 0 < x < d_e, \; a_e = 0, b_e = 0. \tag{7}$$

$$t > 0, x = 0 \quad \frac{\partial a_e(x,t)}{\partial x} = 0, b_e = 0. \tag{8}$$

$$t > 0, x = d_e, \; a_e = a_{e_0}, \; b_e = 0. \tag{9}$$

For diffusion

$$t = 0, d_e \ < x < d_e + d_d \ \ a_d = 0, b_d = 0. \tag{10}$$

$$t > 0, x = d_e \ \ a_d = \ \ a_{d_0}, b_d = \ \ b_{d_0}. \tag{11}$$

$$t > 0, x = d_e + d_d \ \ a_d = \ \ a_{d_1}, \ \frac{\partial b_d(x,t)}{\partial x} = 0. \tag{12}$$

The current density I of the product b on the electrode is $I = \lim_{n\to\infty} i(t)$

$$\text{i(t)} = n_e \ \text{F} \ D_{b_e}\left(\frac{\partial b_e(x,t)}{\partial x}\right) \text{ at } \text{x} = 0. \tag{13}$$

Here i(t) denotes the time dependent current density.

The non-dimensional form using the following dimensionless parameters:

$$U = \ \frac{a}{K_M}, V = \ \frac{b}{K_M}, \chi = \frac{x}{d_e}, \tau \ = \frac{tD}{{d_e}^2}, \ \delta = \frac{d_d}{d_e}, \ u_0 = \frac{a_0}{K_M}, v_0 = \ \frac{b_0}{K_M}, r = \ \frac{D_b}{D_a}, \alpha \ = \ \frac{E_1 \ \ d^2}{D}, \beta = \frac{E_2 \ \ d^2}{D}, \ \varphi^2 = \frac{V_{max} d^2}{D K_M} \tag{14}$$

Where U (χ, τ), V (χ, τ) are the dimensionless accumulation of the substrate, product respectively. χ is the dimensionless distance, τ stands for the dimensionless time, δ is the relative thickness. Let r be a ratio between finite diffusion coefficient, α and β are the ratio between degradation of relative thickness and diffusion coefficient, φ^2 is the Thiele modulus.

Using equation (14), we get equations (3) to (6) in dimensionless form as follows

$$\frac{\partial U_e(\chi,\tau)}{\partial \tau} \ = \ \frac{\partial^2 U_e(\chi,\tau)}{\partial \chi^2} \ - \ \alpha U_e(\chi,\tau) - \ \frac{\varphi^2 U_e(\chi,\tau)}{1+U_e(\chi,\tau)} \tag{15}$$

$$\frac{\partial V_e(\chi,\tau)}{\partial \tau} \ = \ \frac{\partial^2 V_e(\chi,\tau)}{\partial \chi^2} \ - \ \beta \ V_e(\chi,\tau) + \ \frac{\varphi^2 U_e(\chi,\tau)}{1+U_e(\chi,\tau)} \ \ 0 \ < \chi < 1 \tag{16}$$

The initial and boundary conditions are:

$$\tau = 0, 0 \ \ < \chi < 1 \ \ U_e = 0, V_e = 0.$$

$$\chi = 0 \ \ \frac{\partial U_e(\chi,\tau)}{\partial \chi} = 0, V_e = 0.$$

$$\chi = 1 \ \ U_e = u_{e_0}, \ \ V_e = 0. 0 < \chi < 1 \tag{17}$$

$$\frac{\partial U_d(\chi,\tau)}{\partial \tau} \ = \ \frac{\partial^2 U_d(\chi,\tau)}{\partial \chi^2} \ - \ \alpha U_d \ \ (\chi,\tau) \tag{18}$$

$$\frac{\partial V_d(\chi,\tau)}{\partial \tau} \ = \ \frac{\partial^2 V_d(\chi,\tau)}{\partial \chi^2} \ - \ \beta \ \ V_d \ \ (\chi,\tau) \ \ 1 < \chi < 1 + \delta \tag{19}$$

The initial and boundary conditions are:

$$\tau = 0, 1 < \chi < 1 + \delta \ \ U_d = 0, V_d = 0.$$

$$\chi = 1 \ \ U_d = u_{d_0}, V_d = v_{d_0}.$$

$$\chi = 1 + \delta \ \ U_d = u_{d_1}, \ \frac{\partial V_d(\chi,\tau)}{\partial \chi} = 0. \tag{20}$$

The dimensionless current is

$$\psi(t) \ = \frac{I}{n_e \ \text{F} \ D_{V_e}} = \frac{\partial V_e(\chi,\tau)}{\partial \chi} \text{ at } \chi = 0. \tag{21}$$

3. Analytical Expression for the Concentration with Degradation Using New Homotopy Perturbation Method

Asymptotic methods such as the variational iteration method, Adomian decomposition method, Homotopy analysis method, Homotopy perturbation method, and the new approach to Homotopy perturbation to get approximation analytic solutions to non-linear differential equations, the newly developed Homotopy perturbation method is applied for non-linear differential equations [10-15]. In analytical and semi-analytic techniques to nonlinear partial differential equations, the Homotopy analysis method ability to readily demonstrate the convergence of the series solution is unique. Compared to all other techniques, the new Homotopy perturbation method provides a more straightforward approximate solution in the zeroth iteration alone. This approach does not require a small system parameter, making it useful for a wide range of non-linear differential equation solutions. Numerous authors have recently used the new homotopy perturbation method (NHPM) to tackle the non-linear boundary value issue in physics and engineering sciences [16-27].

Using this method (Refer Appendix I), we get the approximate expressions (15) to (19) as follows

$$U_e(\chi,\tau) \ = \frac{B \cos h\sqrt{m+\alpha} \ \ \chi}{\varphi^2 \cos h\sqrt{m+\alpha}} \ - \frac{4\pi B \sum_{n=0}^{\infty}(-1)^n(2\text{n} \ + \ 1)\cos(\frac{\pi}{2})(2\text{n} \ + \ 1)\chi e^{-\ \tau/4(A)}}{\varphi^2 A} \tag{22}$$

$$V_e(\chi,\tau) = \ \frac{B \cos h\sqrt{\beta} \ \ \chi}{\cos h\sqrt{m+\alpha}(m-\beta)} - \ \frac{4\pi B \sum_{n=0}^{\infty}(-1)^n(2\text{n} \ + \ 1)\cos h\sqrt{\frac{4\beta-A}{4}} \ \chi e^{-\ \tau/4(A)}}{(A)(m-\beta)} + \ \frac{B \sin h\sqrt{\beta} \ \ \chi}{\sin h\sqrt{\beta} \ \ (m-\beta)} - \frac{B \sin h\sqrt{\beta} \ \ \chi \cos h\sqrt{\beta}}{\sin h\sqrt{\beta} \ \ (m-\beta)\cos h\sqrt{m+\alpha}}$$

$$-\frac{B\cos h\sqrt{m+\alpha}\ \chi}{\cos h\sqrt{m+\alpha}(m-\beta)}+\frac{4\pi B\sum_{n=0}^{\infty}(-1)^n(2n\ +\ 1)\cos(\frac{\pi}{2})(2n\ +\ 1)\chi e^{-\ \tau/4(A)}}{(A)(m-\beta)}+\frac{4\pi B\sum_{n=0}^{\infty}(-1)^n(2n\ +\ 1)\cos h\sqrt{\frac{4\beta-A}{4}}\ \sin h\sqrt{\frac{4\beta-A}{4}}\ \chi e^{-\ \tau/4(A)}}{(A)(m-\beta)\sin h\sqrt{\frac{4\beta-A}{4}}}$$

$$+\frac{B\sum_{n=0}^{\infty}(-1)^n(2\pi n)\sin n\ \pi\ \chi e^{-((\frac{n\pi}{\delta})^2+B)\tau}}{((n\pi)^2+\beta)(m-\beta)}-\frac{B\sum_{n=0}^{\infty}(-1)^n(2\pi n)\sin n\ \pi\ \chi e^{-((\frac{n\pi}{\delta})^2+\frac{B}{m})\tau}}{((n\pi)^2+\beta)(m-\beta)\cos h\sqrt{m-((n\pi)^2+\beta)}} \tag{23}$$

Where A= $\pi^2(2n+1)^2+4m+4\alpha$, B = mu_{e_0} and $m=\frac{\varphi^2}{2}$.

$$U_d(\chi,\tau)=u_{d_0}\frac{\sin h\left(\sqrt{\alpha}\ \chi-\sqrt{\alpha}(1+\delta)\right)}{\sin h\sqrt{\alpha}(\delta)}-\frac{u_{d_0}\delta\ \sum_{n=0}^{\infty}(-1)^n(2\pi n)\sin(C\ \chi-C(1+\delta))e^{-((C)^2+\alpha)\tau}}{(C)^2+\alpha}$$

$$+\frac{u_{d_1}\sin h\left(\sqrt{\alpha}\ -\sqrt{\alpha}(\chi)\right)}{\sin h\left(\sqrt{\alpha}(\delta)\right)}+\frac{u_{d_1}\delta\ \sum_{n=0}^{\infty}(-1)^n(2\pi n)\sin(C\ -C(\chi))e^{-((C)^2+\alpha)\tau}}{(C)^2+\alpha} \tag{24}$$

Where C = $\frac{n\pi}{\delta}$

$$V_d(\ \chi,\tau)=\frac{v_{d_0}\cos h\sqrt{\beta}(\ \chi-1-\delta)}{\cos h\sqrt{\beta}(\delta)}-\frac{4\pi v_{d_0}\delta^2\sum_{n=0}^{\infty}(-1)^n(2n\ +\ 1)\cos(\frac{\pi}{2(\delta)})(2n\ +\ 1)(\chi-1-\delta)e^{-\frac{\tau(\pi^2(2n+1)^2+4\beta\delta^2)}{4\delta^2}}}{\pi^2(2n+1)^2+4\beta\delta^2} \tag{25}$$

Using equations (21) and (23), The current expression for non steady state case is

$$\psi(t)=\frac{B\sqrt{\beta}}{\sin h\sqrt{\beta}\ (m-\beta)}-\frac{B\sqrt{\beta}\cos h\sqrt{\beta}}{\sin h\sqrt{\beta}\ (m-\beta)\cos h\sqrt{m+\alpha}}+\frac{B\sum_{n=0}^{\infty}(-1)^n(2(n\pi)^2)e^{-((\frac{n\pi}{\delta})^2+B)\tau}}{((n\pi)^2+\beta)(m-\beta)}-\frac{B\sum_{n=0}^{\infty}(-1)^n(2(n\pi)^2)e^{-((\frac{n\pi}{\delta})^2+\frac{B}{m})\tau}}{((n\pi)^2+\beta)(m-\beta)\cos h\sqrt{m-((n\pi)^2+\beta)}}+$$
$$\frac{4\pi B\sum_{n=0}^{\infty}(-1)^n(2n\ +\ 1)\cos h(\sqrt{\frac{4\beta-A}{4}})\ \sqrt{\frac{4\beta-A}{4}}e^{-\frac{\tau(A)}{4}}}{(A)(m-\beta)\sin h\sqrt{\frac{4\beta-A}{4}}} \tag{26}$$

When $\tau\to\infty$ equation (26) becomes

$$\psi(s)=\frac{B\sqrt{\beta}}{\sin h\sqrt{\beta}\ (m-\beta)}-\frac{B\sqrt{\beta}\cos h\sqrt{\beta}}{\sin h\sqrt{\beta}\ (m-\beta)\cos h\sqrt{m+\alpha}} \tag{27}$$

Equations (27) is called the current expression for steady state case.

Where A= $\pi^2(2n+1)^2+4m+4\alpha$, B = mu_{e_0} and $m\ =\ \frac{\varphi^2}{2}$

4. Limiting Cases

This section derived analytical expressions for the concentration of substrate, product and current for special cases.

4.1. Case 1: When the Rate of Substrate Degradation $\alpha=0$

Suppose we consider initially, when the rate of degradation substrate $\alpha=0$ and then the Eqn. (15) & (18) reduced to be as follows [27-30],

$$\frac{\partial U_e(\chi,\tau)}{\partial\tau}\ =\ \frac{\partial^2U_e(\chi,\tau)}{\partial\chi^2}\ -\ \frac{\varphi^2U_e(\chi,\tau)}{1+U_e(\chi,\tau)}\quad 0<\chi<1 \tag{28}$$

$$\frac{\partial U_d(\chi,\tau)}{\partial\tau}\ =\ \frac{\partial^2U_d(\chi,\tau)}{\partial\chi^2}\quad 1<\chi<1+\delta \tag{29}$$

Using (17) and (20) boundary conditions for the above equation can be found the analytical expressions derived in (Refer Appendix II) as,

$$U_e(\chi,\tau) = \frac{u_{e_0}\cos h\sqrt{m}\ \chi}{\cos h\sqrt{m}} - \frac{4\pi u_{e_0}\sum_{n=0}^{\infty}(-1)^n(2n\ +\ 1)\cos^{\pi}/_2(2n\ +\ 1)\chi e^{-\ \tau/_4(\pi^2(2n+1)^2+4m)}}{(\pi^2(2n+1)^2+4m)} \tag{30}$$

$$U_d(\chi,\tau) = \frac{u_{d_1}\delta\ \sum_{n=0}^{\infty}(-1)^n(2\pi n)\sin(C\ -C(\chi))e^{-((C)^2)\tau}}{(C)^2} - \frac{u_{d_0}\delta\ \sum_{n=0}^{\infty}(-1)^n(2\pi n)\sin(C\ \chi-C(1+\delta))e^{-((C)^2)\tau}}{(C)^2} \tag{31}$$

Where C= $\frac{n\pi}{\delta}$ & $m = \frac{\varphi^2}{2}$

4.2. Case 2: When the Rate of Product Degradation $\beta = 0$

Suppose we consider initially, when the rate of degradation product $\beta = 0$ and then the Eqn. (16) & (19) reduced to be as follows [27-30],

$$\frac{\partial V_e(\chi,\tau)}{\partial\tau} = \frac{\partial^2 V_e(\chi,\tau)}{\partial\chi^2} + \frac{\varphi^2 U_e(\chi,\tau)}{1+U_e(\chi,\tau)} \quad 0<\chi<1 \tag{32}$$

$$\frac{\partial V_d(\chi,\tau)}{\partial\tau} = \frac{\partial^2 V_d(\chi,\tau)}{\partial\chi^2} \quad 1<\chi<1+\delta \tag{33}$$

Using (17) and (20) boundary conditions for the above equation can be found the analytical expressions derived in (Refer Appendix III) as,

$$V_e(\chi,\tau) = \frac{B}{\cos h\sqrt{m+\alpha}(m)} - \frac{4\pi B\sum_{n=0}^{\infty}(-1)^n(2n\ +\ 1)\cos h\sqrt{\frac{(-A)}{4}}\ \chi e^{-\ \tau/_4(A)}}{(A)(m)}$$

$$-\frac{B\cos h\sqrt{m+\alpha}\ \chi}{\cos h\sqrt{m+\alpha}(m)} + \frac{4\pi B\sum_{n=0}^{\infty}(-1)^n(2n\ +\ 1)\cos(\frac{\pi}{2})(2n\ +\ 1)\chi e^{-\ \tau/_4(A)}}{(A)(m)}$$

$$+\frac{4\pi B\sum_{n=0}^{\infty}(-1)^n(2n\ +\ 1)\cos h\sqrt{\frac{(-A)}{4}}\ \sin h\sqrt{\frac{(-A)}{4}}\ \chi e^{-\ \tau/_4(A)}}{(A)(m)\sin h\sqrt{\frac{(-A)}{4}}}$$

$$+\frac{B\sum_{n=0}^{\infty}(-1)^n(2\pi n)\sin n\pi\ \chi e^{-((\frac{n\pi}{\delta})^2+B)\tau}}{((n\pi)^2)(m)} - \frac{B\sum_{n=0}^{\infty}(-1)^n(2\pi n)\sin n\pi\ \chi e^{-((\frac{n\pi}{\delta})^2+\frac{B}{m})\tau}}{((n\pi)^2)(m)\cos h\sqrt{m-((n\pi)^2)}} \tag{34}$$

$$V_d(\ \chi,\tau) = v_{d_0} - \frac{4\pi v_{d_0}\delta^2\sum_{n=0}^{\infty}(-1)^n(2n\ +\ 1)\cos(\frac{\pi}{2(\delta)})(2n\ +\ 1)(\chi-1-\delta)e^{-\ \frac{\tau(\pi^2(2n+1)^2)}{4\delta^2}}}{\pi^2(2n+1)^2} \tag{35}$$

$$\psi(t) = \frac{B\sum_{n=0}^{\infty}(-1)^n(2(n\pi)^2)e^{-((\frac{n\pi}{\delta})^2+B)\tau}}{((n\pi)^2)(m)} - \frac{B\sum_{n=0}^{\infty}(-1)^n(2(n\pi)^2)e^{-((\frac{n\pi}{\delta})^2+\frac{B}{m})\tau}}{((n\pi)^2)(m)\cos h\sqrt{m-((n\pi)^2)}} + \frac{4\pi B\sum_{n=0}^{\infty}(-1)^n(2n\ +\ 1)\cos h(\sqrt{\frac{(-A)}{4}})\ \sqrt{\frac{(-A)}{4}}e^{-\ \frac{\tau(A)}{4}}}{(A)(m)\sin h\sqrt{\frac{(-A)}{4}}} \tag{36}$$

Where

$$\text{A}= \pi^2(2n+1)^2+4m+4\alpha,\ \text{B} = mu_{e_0} \text{ and } m = \frac{\varphi^2}{2}. \tag{37}$$

4.3. Case 3: When the Rate of Substrate and Product Degradation $\alpha = \beta = 0$

In this case, when the rate of degradation of substrate and product $\alpha = \beta = 0$ and the two-compartment model was reduced to the one compartment model when $\delta = 0$. Therefore the Eqn. (14) and (15) can be reduced to

$$\frac{\partial U_e(\chi,\tau)}{\partial\tau} = \frac{\partial^2 U_e(\chi,\tau)}{\partial\chi^2} - \frac{\varphi^2 U_e(\chi,\tau)}{1+U_e(\chi,\tau)} \tag{38}$$

$$\frac{\partial V_e(\chi,\tau)}{\partial\tau} = \frac{\partial^2 V_e(\chi,\tau)}{\partial\chi^2} + \frac{\varphi^2 U_e(\chi,\tau)}{1+U_e(\chi,\tau)} \quad 0\ <\chi<1 \tag{39}$$

The initial and boundary conditions are:

$$\tau = 0, 0 \quad < \chi < 1 \quad U_e = 0, V_e = 0.$$

$$\chi = 0 \quad \frac{\partial U_e(\chi,\tau)}{\partial \chi} = 0, V_e = 0.$$

$$\chi = 1 \quad U_e = u_{e_0}, \quad V_e = 0. 0 < \chi < 1 \tag{40}$$

5. Analytical Expression for the Concentration Without Degradation Using Akbari-Ganji Method

The Akbari-Ganji method approach is an excellent analytical solution technique for nonlinear differential equations. First, a polynomial is assumed to be the solution to the equation. Then, an algebraic system of equations is constructed based on the boundary or initial conditions, from which the assumed constant coefficients of polynomials are obtained upon solving the system of equations. In this case, the above equations can be solved the approximate analytical expressions for concentrations and current under the steady state condition using the Akbari-Ganji method as follows (Refer Appendix IV) [17-26],

$$U_e(\chi) = \frac{u_{e_0}}{\cos h L_1} \cos h \quad L_1 \chi \tag{41}$$

$$V_e(\chi) = 1 - \cos h \quad M_1 \chi + \frac{(\cosh M_1 - 1) \ \sin h M_1 \chi}{\sin h M_1} \tag{42}$$

Where

$$L_1 = \varphi \sqrt{\frac{1}{1+u_{e_0}}}, \quad M_1 = \varphi \sqrt{\frac{u_{e_0}}{1+u_{e_0}}} \tag{43}$$

The steady-state current becomes using (21).

$$I = \frac{(\cosh M_1 - 1)}{\sin h M_1} . M_1 \tag{44}$$

$$\text{Where } M_1 = \varphi \sqrt{\frac{u_{e_0}}{1+u_{e_0}}} \tag{45}$$

6. Comparision of Analytical Results and Numerical Simulations

Numerical simulations are used to compare the analytical results, which are presented in the following Tables. The Numerical simulations are presented in (Refer Appendix V) using pdex4 function in MATLAB. Equations (22) to (25) are the simple approximate analytical expressions for the substrate (U_e , U_d) and product (V_e, V_d) concentrations in two layers.

Table 1. *For various values of the parameter* φ^2 *and some certain values of the parameter* $\alpha = 61, \tau = 1, u_{e_0} = 1$ *in Eqn. (22). The similarity relation between substrate concentration* U_e *and numerical result.*

χ	$\varphi^2 = 3$			$\varphi^2 = 5$			$\varphi^2 = 25$		
	Numerical	U_e **in eqn. (22)**	**% of deviation**	**Numerical**	U_e **in eqn. (22)**	**% of deviation**	**Numerical**	U_e **in eqn. (22)**	**% of deviation**
0	0	0	0	0	0	0	0	0	0
0.2	0.002	0.001		0.001	0.001	0.00	0	0	0
0.4	0.008	0.008	0	0.008	0.008	0.00	0.004	0.004	0
0.6	0.043	0.043	0	0.044	0.043	0.04	0.027	0.026	3.70
0.8	0.217	0.218	0.46	0.227	0.217	0.21	0.178	0.171	3.93
1	1	1	0	1	1	0	1	1	0
	Average percentage error: 0.07			Average percentage error: 0.041			Average percentage error: 1.272		

Table 2. *For different values of the parameter* φ^2 *and some certain values of the parameter* $\alpha = 50, \beta = 310, \tau = 1, u_{e_0} = 1$ *in eqn. (23). The similarity relation between product concentration* V_e *and numerical result.*

χ	$\varphi^2 = 3.5$			$\varphi^2 = 12.5$			$\varphi^2 = 100$		
	Numerical	**V_e in eqn. (23)**	**% of deviation**	**Numerical**	**V_e in eqn. (23)**	**% of deviation**	**Numerical**	**V_e in eqn. (23)**	**% of deviation**
0	0.000	0.000	0.000	0.000	0.000	0.000	0.000	0.000	0.000
0.2	0.000	0.000	0.000	0.000	0.000	0.000	0.000	0.000	0.000
0.4	0.000	0.000	0.000	0.000	0.000	0.000	0.000	0.000	0.000
0.6	0.000	0.000	0.000	0.000	0.000	0.000	0.000	0.020	3.000
0.8	0.002	0.001	0.5	0.002	0.003	0.5	0.002	0.008	3.200
1	1	1	0.000	1	1	0	1	1	0.000
	Average percentage error: 0.083			Average percentage error: 0.083			Average percentage error: 1.960		

Table 3. *For various values of the parameter* α *and some fixed values of the parameter* $\tau = 1,\ \delta = 0.1, u_{d_0} = 1, u_{d_1}$*=1 in substrate concentration* U_d *from Eqn. (24) is given to differentiate numerical result.*

χ	$\alpha = 20$			$\alpha = 40$			$\alpha = 60$		
	Numerical	**U_d in eqn. (24)**	**% of deviation**	**Numerical**	**U_d in eqn. (24)**	**% of deviation**	**Numerical**	**U_d in eqn. (24)**	**% of deviation**
1	1	1	0.00	1	1	0.00	1	1	0
1.02	0.984	0.984	0.00	0.969	0.969	0.00	0.956	0.958	0.20
1.04	0.976	0.976	0.00	0.954	0.954	0.00	0.934	0.935	0.10
1.06	0.976	0.976	0.00	0.954	0.954	0.00	0.934	0.935	0.10
1.08	0.984	0.984	0.00	0.969	0.969	0.00	0.957	0.958	0.10
1.1	1	1	0.00	1	1	0.00	1	1	0
	Average percentage error: 0.00			Average percentage error: 0.00			Average percentage error: 0.08		

Table 4. *Comparison of diffusion product concentration* V_d *in eqn. (25) with numerical result for several values of the parameter* β *and some certain values of the parameter* $\delta = 0.2, v_{d_0} = 1,\ \tau = 1.$

χ	$\beta = 90$			$\beta = 145$			$\beta = 300$		
	Numerical	**V_d in eqn. (25)**	**% of deviation**	**Numerical**	**V_d in eqn. (25)**	**% of deviation**	**Numerical**	**V_d in eqn. (25)**	**% of deviation**
1	1	1	0	1	1	0	1	1	0
1.05	0.648	0.641	1.080	0.547	0.548	0.182	0.418	0.418	0
1.1	0.439	0.432	1.594	0.31	0.313	0.967	0.179	0.179	0
1.15	0.325	0.325	0	0.195	0.202	3.589	0.084	0.085	1.190
1.2	0.282	0.293	3.900	0.168	0.171	1.785	0.06	0.062	3.333

χ	$\beta = 90$			$\beta = 145$			$\beta = 300$		
	Numerical	V_d **in eqn. (25)**	**% of deviation**	**Numerical**	V_d **in eqn. (25)**	**% of deviation**	**Numerical**	V_d **in eqn. (25)**	**% of deviation**
	Average percentage error: 1.314			Average percentage error: 1.304			Average percentage error: 0.904		

The above Tables 1-4 show that the maximum error between numerical and (NHPM) analytical results for enzyme layer substrate and product is 0.461% and 0.708%, and for diffusion layer substrate and product, it is 0.026% and 1.174% for the parameter values. Therefore error percentage is less than two is obtained from NHPM.

7. Results and Discussion

The similarity relation between the analytical results (NHPM) of substrate concentration $U_e, U_d,$ product concentration V_e, V_d with numerical simulations using Eqn. (22) to (25) and non-dimensional current and all kinetic parameters under steady, non-steady state conditions using eqn. (22) and (27) are presented in the following Figures 1-6.

From Figure 2 (a) and (b), when substrate concentration decreases with increasing the rate of degradation parameter α and thiele modulus φ^2. From Figure 2 (c) plot for various values of τ for some fixed values of $\alpha = 2, \varphi = 3, u_{e_0} = 1$. Thus it is concluded that various values of τ is increases as the substrate (U_e) increases. Figure 3 (a) Various kinetic parameter values of degradation rate β increase as substrate concentration decreases. Then Figure 3 (b) and (c), the substrate increases with the Thiele modulus $\varphi^2$and time increases. Figure 4 (a) represents various values of α increases and concentration decreases. From Figure 4 (b), the plot for several values of τ specific values of of $\alpha = 20, \delta = 0.1, u_{d_0} = 1, u_{d_1}$=1. Thus, it is concluded that various values τ do not change in the substrate (U_d).

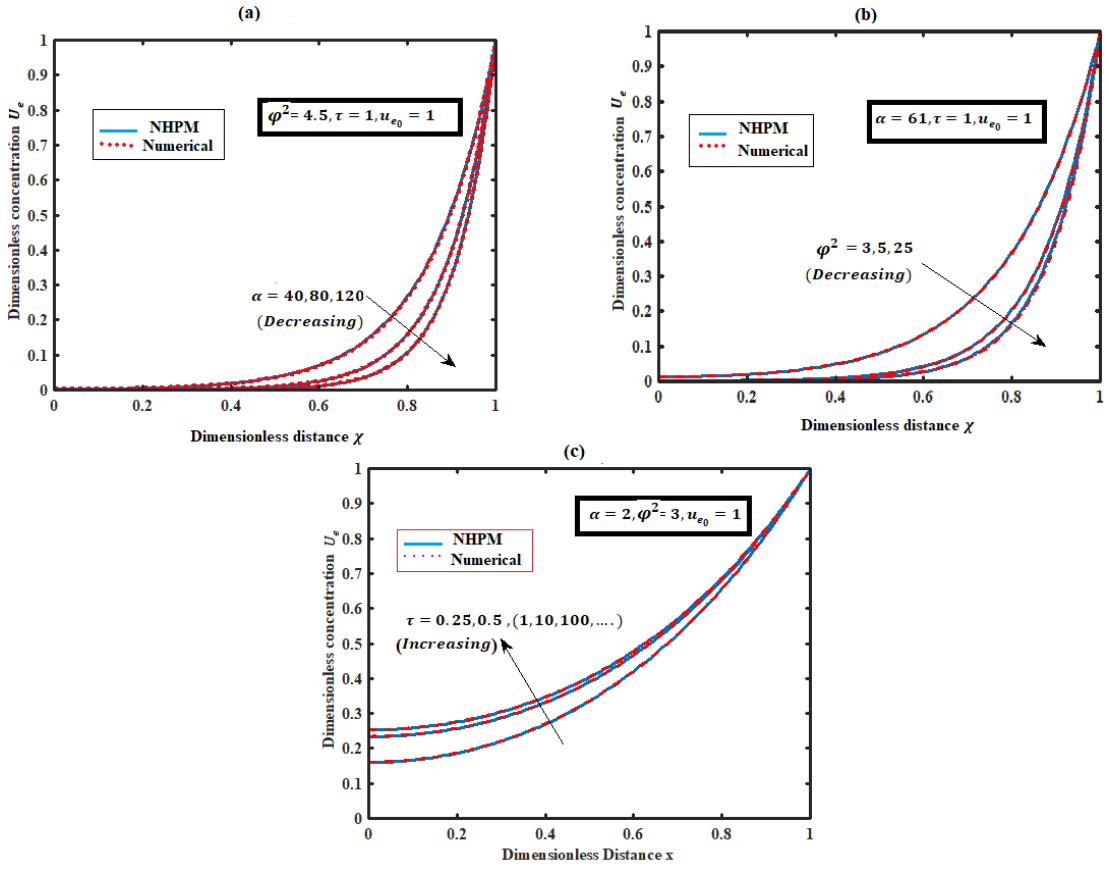

Figure 2. *Substrate concentration U_e in contrast to Dimensionless distance χ using in eqn. (22) for several values of non dimensional parameter α, φ and τ for certain values of the parameters α, φ, τ and u_{e_0}.*

Figure 5 (a) kinetic parameter β for some specific parameter values $= 0.2, \tau = 1, v_{d_0} = 1$. There is a parameter β increase as the concentration of the product (V_d) decreases.

From Figure 5 (b): plot for several values of τ some specific values $\beta = 130, \delta = 0.1, v_{d_0} = 1$. Thus it is concluded that various values do not change in the product (V_d).

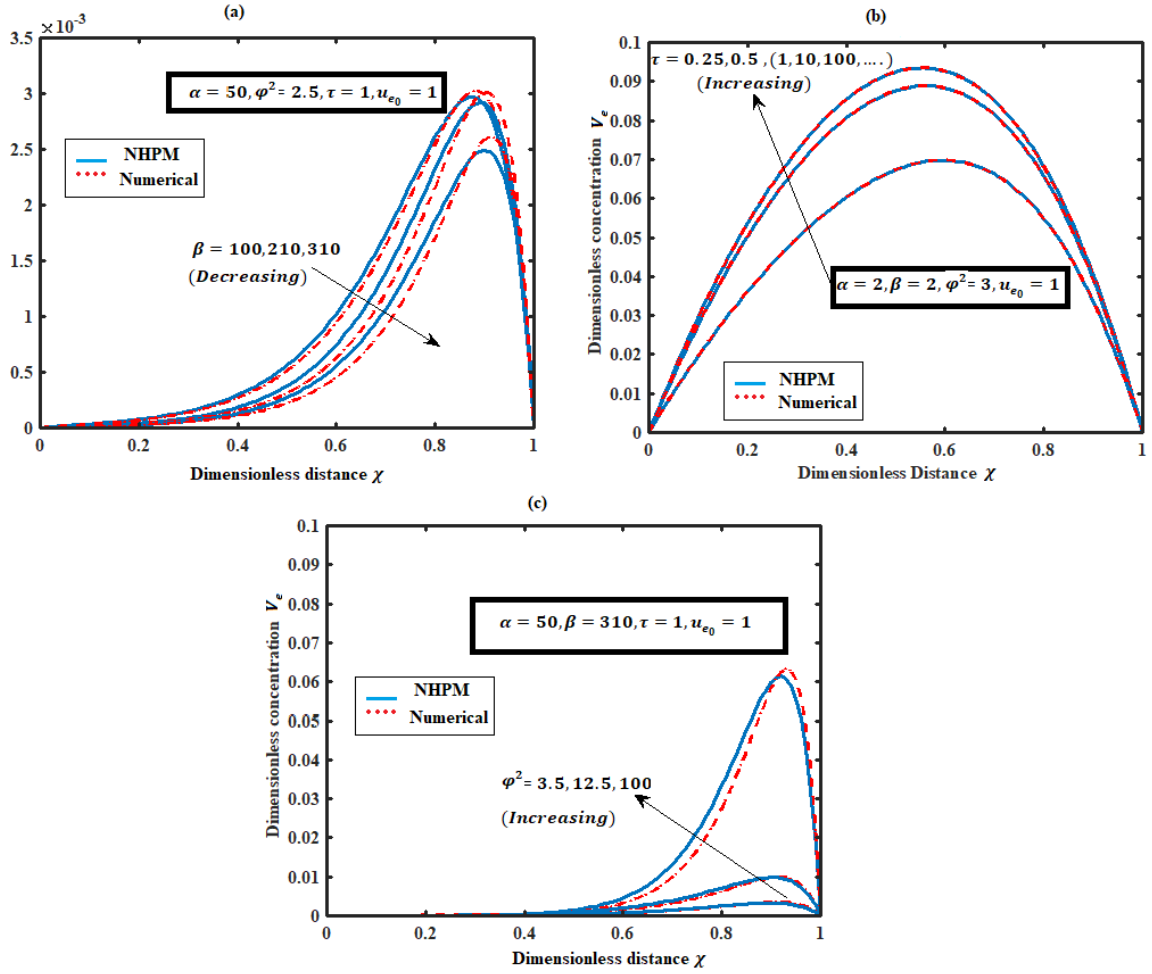

Figure 3. *Product concentration V_e in differentiate to Dimensionless distance χ using in eqn. (23) for different values of non dimensional parameter β, φ^2 and τ for some fixed values of the parameters $\alpha, \beta, \varphi^2, \tau$ and u_{e_0}.*

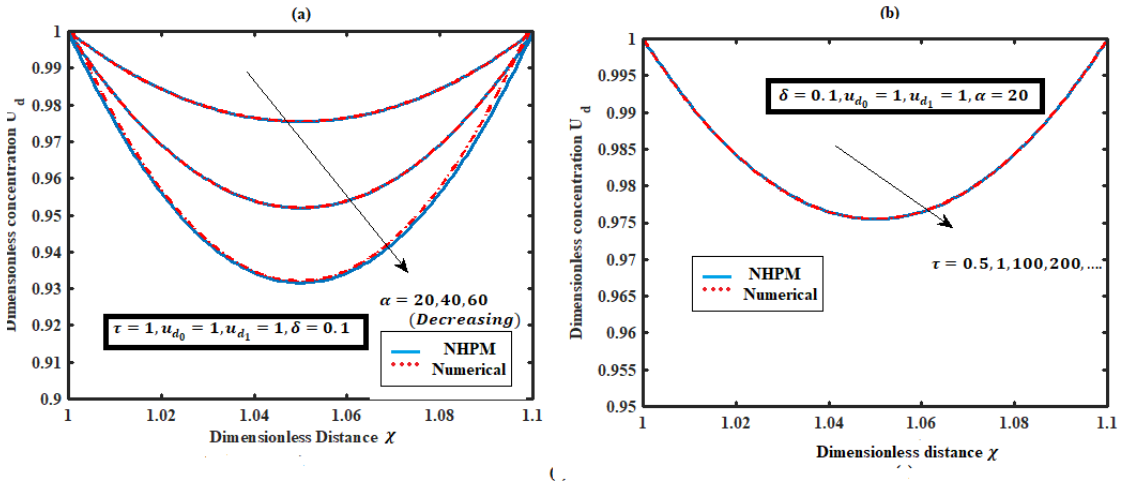

Figure 4. *Substrate concentration U_d is compare to Dimensionless distance χ using in eqn. (24) for several values of non dimensional parameter α, δ and τ for fixed values of the parameters $\alpha, \delta, \tau, u_{d_0}$ and u_{d_1}.*

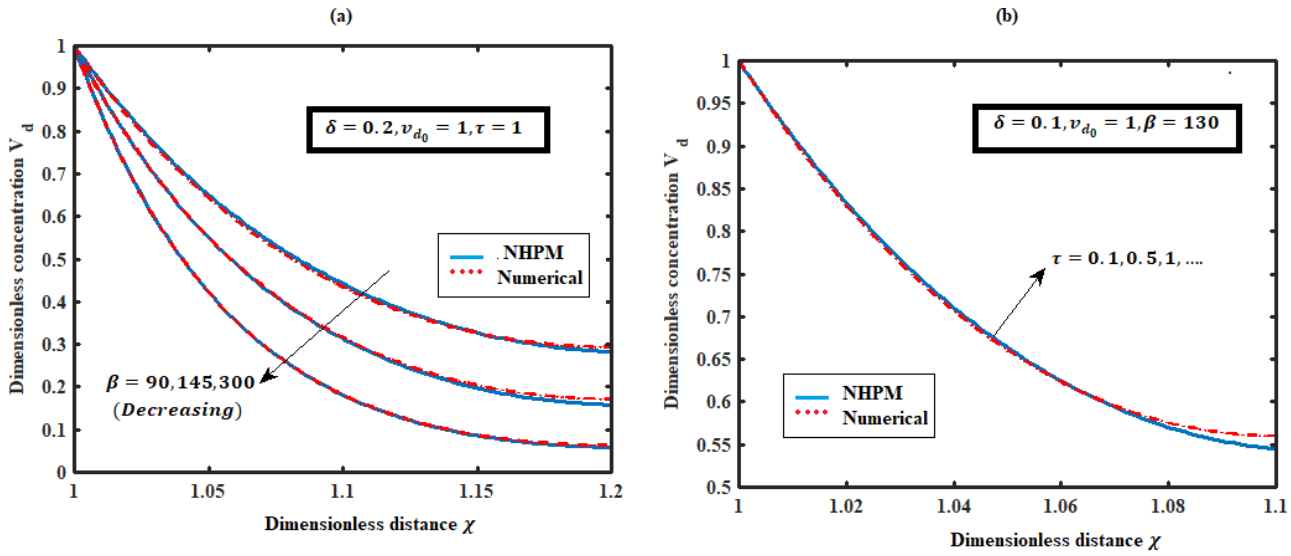

Figure 5. *Product concentration V_d is differentiate to Dimensionless distance χ using in eqn. (25) for several values of non dimensional parameter β, δ and τ for dif ferent values of the parameters β, δ, τ and v_{d_0}.*

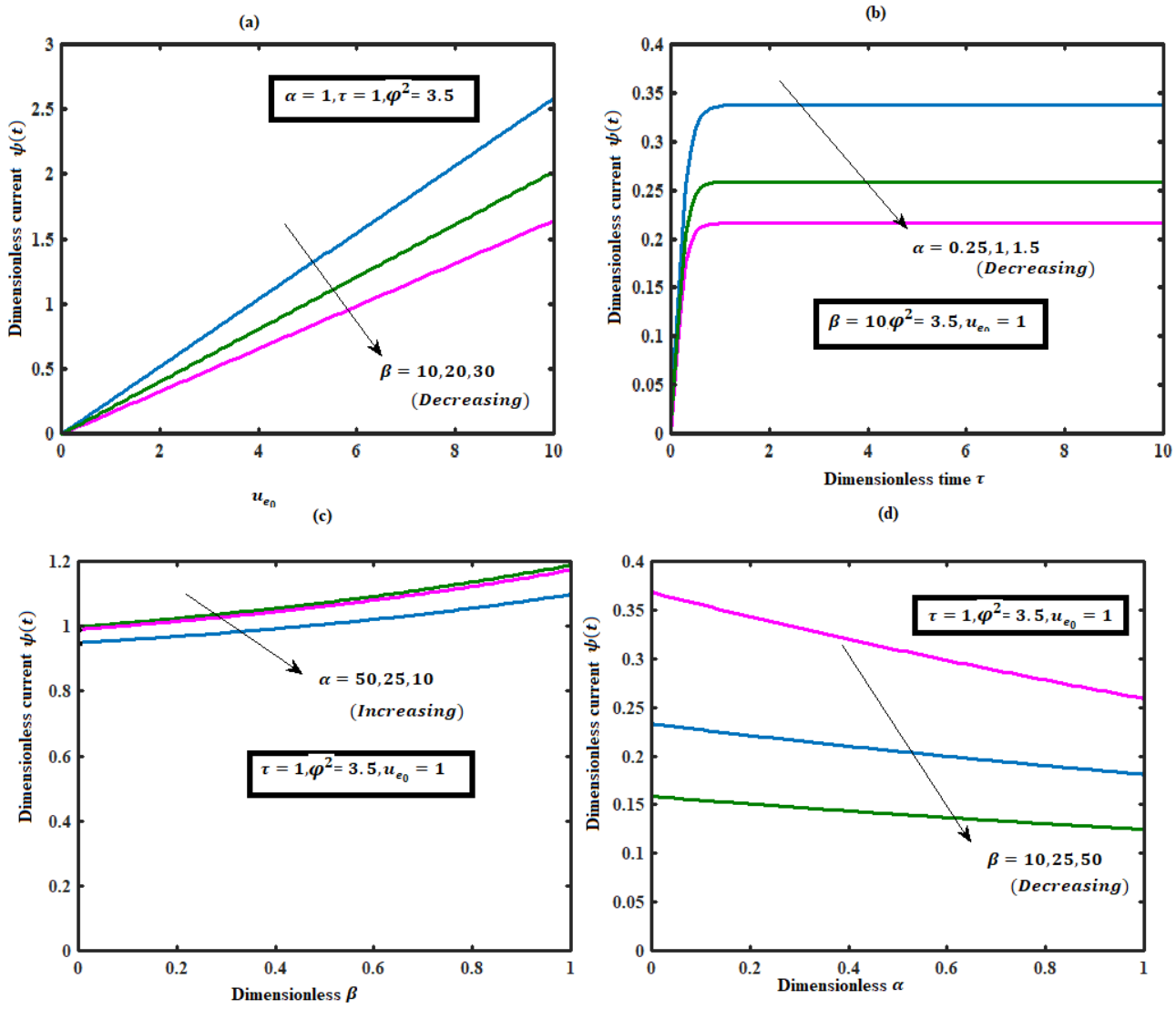

Figure 6. *Dimensionless non steady state current $\psi(t)$ in contrast to non dimensional parameter α, β, τ and u_{e_0} for certain values of the parameters $\alpha, \beta, \varphi^2, \tau$ and u_{e_0} using eqn. (26).*

Figure 6 (a) and (b) exposes parameter $u_{e_0} and\ \tau$ increases with the dimensionless current $\psi(t)$ decreases. Figure 6 (c) represents various values of α some specific values $u_{e_0} = 1, \varphi^2 = 3.5, \tau = 1$. Thus it is concluded that the parameter β increase and the dimensionless current $\psi(t)$ increase. Figure 6 (d) expresses it is clear that non-dimensional parameter α increase as the dimensionless current decreases. Figure 7 (a) & (b) is clear that there are parameter increases as well as dimensionless current $\psi(s)$ increases. Figure 7 (c) expresses the dimensionless current $\psi(s)$ increasing with the thiele modulus φ^2 increases. Stabilizing the sensor components increases degradation to the concentration of substrate and product, decreasing performance in real-world applications.

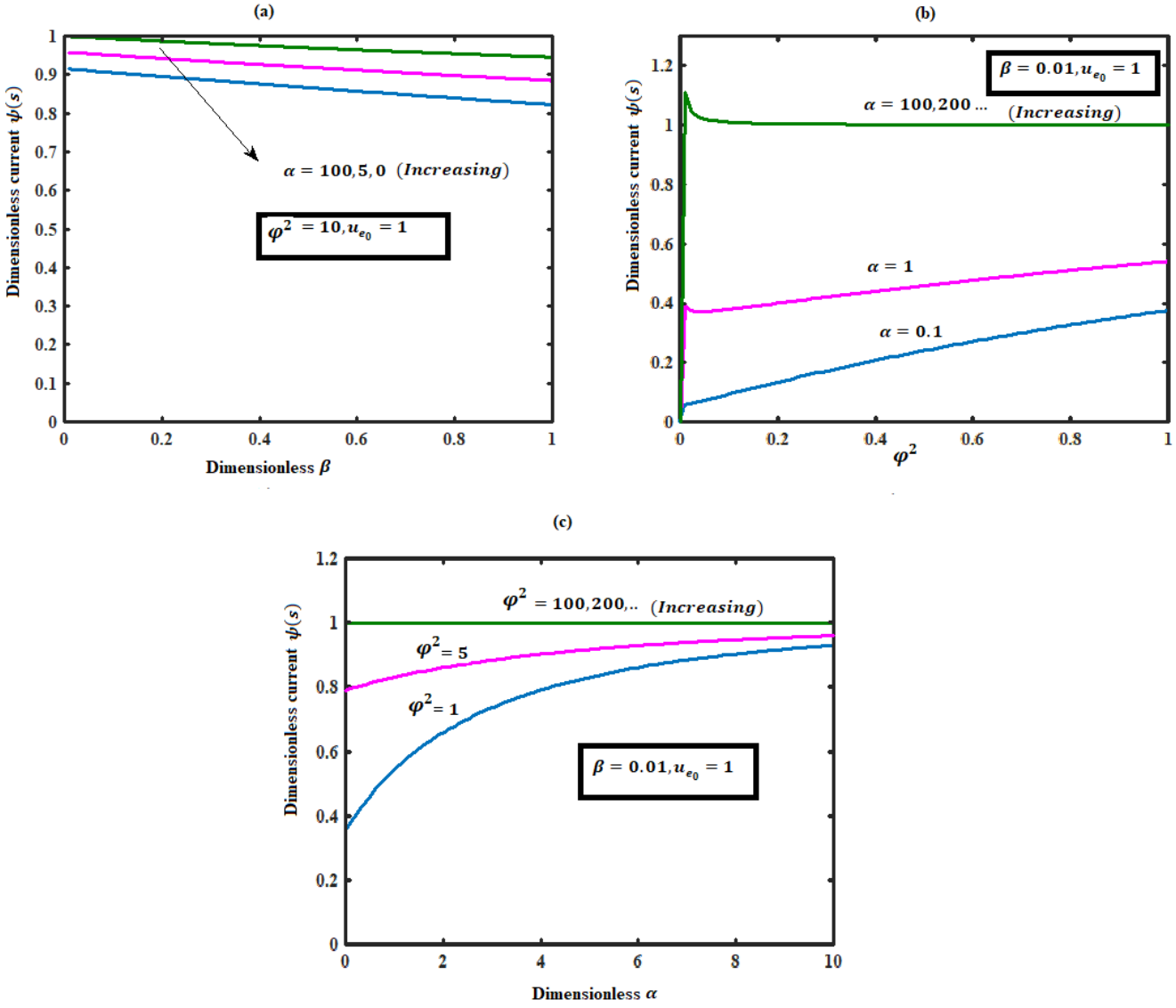

Figure 7. *Dimensionless steady state current $\psi(s)$ in contrast to non dimensional parameter α, β and φ^2 for certain values of the parameters α, β, φ^2 and u_{e_0}.*

Figure 8 (a) and (b) exposes parameter φ^2 increases with the dimensionless concentration of substrate and product decreases using (41) – (43) in limiting case 3.

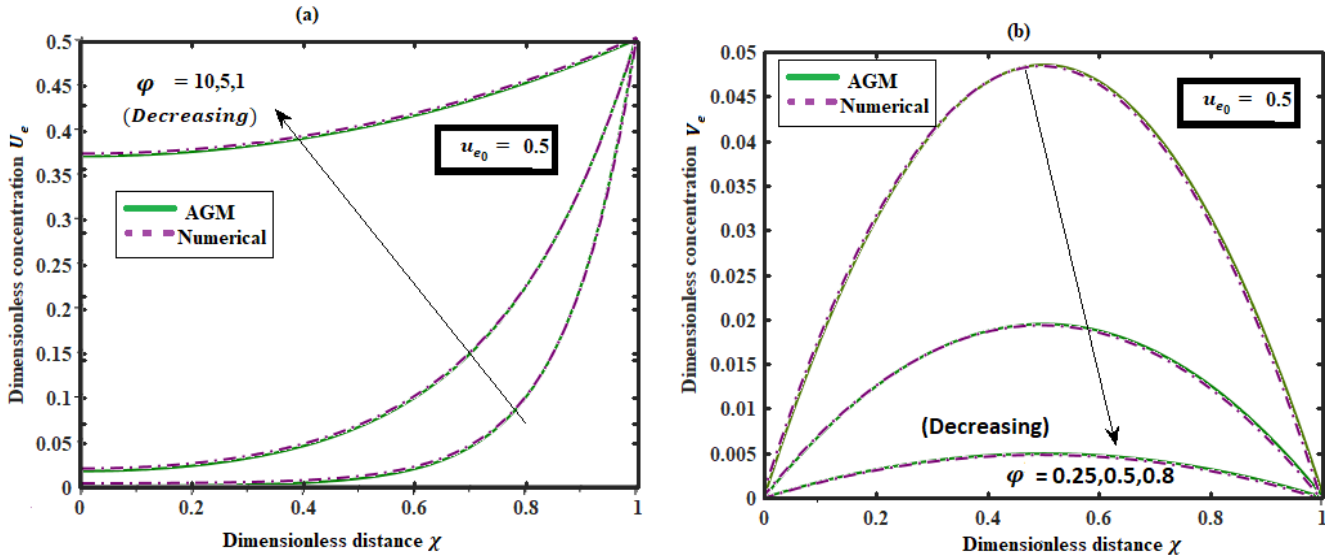

Figure 8. *Dimensionless distance χ in contrast to concentration for certain values of the parameters φ and fixed values of u_{e_0}.*

8. Conclusions

Multilayer heterogeneous biocatalytic systems of nonlinear reaction equations in the diffusion layer and enzymatic mechanism have been analytically solved using the new homotopy perturbation method. This study proposes an approximate analytical expression for the degradation of substrate, product, current, and responsiveness to non-steady-state and steady-state conditions. These expressions are compared with numerical simulations graphically for all values of parameters discussed. It shows that degradation rates of substrate and product increase as the dimensionless concentration of substrate and product for two layers decreases. Stabilizing the sensor components to minimize degradation is crucial for preserving dependable long-term performance in real-world applications. The new homotopy perturbation method is a straightforward and effective method that can solve this nonlinear equation.

Further limiting cases, three situations are created. Three scenarios have led to the creation of profiles showing how the substrate and product degradation rates do not affect the biosensor response. The Akbari-Ganji method (AGM) resolves the third scenario by degradation rates that do not affect the biosensor's response. This method is discussed and compared to numerical simulations, and it is presented graphically. This work may be extended to the three-layer model of nonlinear equations in chemical reactions with similar boundary conditions in steady and non-steady state conditions.

Nomenclature

a_e & a_d	concentration of substrate - enzyme and diffusion layer (mol cm^{-3})
b_e & b_d	concentration of product - enzyme and diffusion layer (mol cm^{-3})
δ	Dimensionless Thickness of the membrane
U	Dimensionless concentration of substrate
V	Dimensionless concentration of product
a_0 & b_0	Initial concentration of species (mol cm^{-3})
d_e & d_d	Thickness of the membrane (cm)
φ^2	Thiele modulus
D	Diffusion coefficient of substrate (cm^2s^{-1})
α & β	Dimensionless degradation rate
t	Time (s)
τ	Dimensionless time
χ	Normalized electrode distance
x	Distance from electrode (cm)

Abbreviations

NHPM	New Homotopy Perturbation Method
AGM	Akbari-Ganji Method

Acknowledgments

The authors thank Dr. R. Swaminathan, Principal of Vidhyaa Giri College of Arts and Science in Puduvayal, for his steadfast encouragement and support.

Author Contributions

Ranjani Kesavan: Conceptualization, Data curation, Formal Analysis, Investigation, Methodology, Software, Validation, Visualization, Writing – original draft, Writing – review & editing

Swaminathan Rajagopal: Conceptualization, Formal Analysis, Project administration, Validation, Visualization

Karpagavalli Ramasamy: Conceptualization, Formal

Analysis, Investigation, Project administration, Resources, Supervision, Validation, Visualization

Conflicts of Interest

The authors declare no conflicts of interest.

Appendix

Appendix I: New Homotopy Perturbation Method

In section 3, Using equations (A-15) to (A-19) to construct new homotopy as follows,

$$(1-p)\left[\frac{\partial^2 U_e(\chi,\tau)}{\partial\chi^2}-\alpha U_e(\chi,\tau)-\frac{\varphi^2 U_e(\chi,\tau)}{(1+U_e)\ ((\chi=1)}-\frac{\partial U_e(\ \chi,\tau)}{\partial\tau}\right]+p\left[\left(1+U_e(\chi,\tau)\right)\left(\frac{\partial^2 U_e(\chi,\tau)}{\partial\chi^2}\ -\alpha U_e(\chi\ \ \tau)-\frac{\partial U_e(\ \chi,\tau)}{\partial\tau}\right)-\varphi^2 U_e(\chi,\tau)\right]=0 \quad \text{(A-1)}$$

$$(1-p)\left[\frac{\partial^2 U_e(\chi,\tau)}{\partial\chi^2}-\alpha U_e(\chi,\tau)-\frac{\varphi^2 U_e(\chi,\tau)}{(1+u_{e_0})\ (u_{e_0}=1)}-\frac{\partial U_e(\ \chi,\tau)}{\partial\tau}\right]+p\left[\left(1+U_e(\chi\ \ \tau)\right)\left(\frac{\partial^2 U_e(\chi,\tau)}{\partial\chi^2}\ -\alpha U_e(\chi,\tau)-\frac{\partial U_e(\ \chi,\tau)}{\partial\tau}\right)-\varphi^2 U_e(\chi,\tau)\right]=0 \quad \text{(A-2)}$$

$$(1-p)\left[\frac{\partial^2 U_e(\chi,\tau)}{\partial\chi^2}-\alpha U_e(\chi,\tau)-\frac{\varphi^2 U_e(\chi,\tau)}{2}-\frac{\partial U_e(\ \chi,\tau)}{\partial\tau}\right]+p\left[\left(1+U_e(\chi\ \ \tau)\right)\left(\frac{\partial^2 U_e(\chi,\tau)}{\partial\chi^2}\ -\alpha U_e(\chi\ \ \tau)-\frac{\partial U_e(\ \chi,\tau)}{\partial\tau}\right)-\varphi^2 U_e(\chi\ ,\tau)\right]=0 \quad \text{(A-3)}$$

Simillarly, the above process of product as follow,

$$(1-p)\left[\frac{\partial^2 V_e(\chi,\tau)}{\partial\chi^2}-\beta V_e(\chi,\tau)+\frac{\varphi^2 U_e(\chi,\tau)}{2}-\frac{\partial V_e(\ \chi,\tau)}{\partial\tau}\right]+p\left[\left(1+U_e(\chi,\tau)\right)\left(\frac{\partial^2 V_e(\chi,\tau)}{\partial\chi^2}\ -\beta V_e(\chi,\tau)-\frac{\partial V_e(\ \chi,\tau)}{\partial\tau}\right)+\varphi^2 U_e(\chi,\tau)\right]=0 \quad \text{(A-4)}$$

The approximate solutions of (A-3) and (A-4) are

$$U_e=U_{e_0}+p\ U_{e_1}\ +p^2U_{e_2}\ \ +p^3U_{e_3}+\cdots\ldots\cdot \quad \text{(A-5)}$$

$$V_e=V_{e_0}+p\ V_{e_1}\ +p^2V_{e_2}\ \ +p^3V_{e_3}+\cdot\ \cdot \quad \text{(A-6)}$$

Equating the coefficients of p and substituting Equations (A-5) and (A-6) into Equations (A-3) and (A-4)

$$p^0:\ \frac{\partial^2 U_{e_0}\ (\chi,\tau)}{\partial\chi^2}-\alpha U_{e_0}\ -\frac{\varphi^2 U_{e_0}}{2}-\frac{\partial U_{e_0}\ (\ \chi,\tau)}{\partial\tau}=0 \quad \text{(A-7)}$$

$$p^0:\ \frac{\partial^2 V_{e_0}\ (\chi,\tau)}{\partial\chi^2}-\beta\ V_{e_0}\ +\frac{\varphi^2 U_{e_0}}{2}-\frac{\partial V_{e_0}\ (\ \chi,\tau)}{\partial\tau}=0 \quad \text{(A-8)}$$

The boundary conditions are:

$$\chi=0\ \ \frac{\partial U_{e_0}\ (\chi,\tau)}{\partial\chi}=0, V_{e_0}\ =0.$$

$$\chi=1\ \ U_{e_0}\ =u_{e_0},\ V_{e_0}\ =0. \quad \text{(A-9)}$$

Taking Laplace transform in (A-7) to (A-9),

$$p^0:\ \frac{\partial^2\overline{U_{e_0}}}{\partial\chi^2}-\alpha\overline{U_{e_0}}\ -m\overline{U_{e_0}}\ -s\overline{U_{e_0}}=0 \quad \text{(A-10)}$$

$$p^0:\ \frac{\partial^2\overline{V_{e_0}}}{\partial\chi^2}-\beta\overline{V_{e_0}}\ +m\overline{U_{e_0}}\ -s\overline{V_{e_0}}=0 \quad \text{(A-11)}$$

The boundary conditions become:

$$\chi = 0 \quad \frac{\partial \overline{U_{e_0}}\ (0)}{\partial \chi} = 0, \overline{V_{e_0}}\ (0)\ = 0.$$

$$\chi = 1 \quad \overline{U_{e_0}}\ = \frac{u_{e_0}}{s}, \ \overline{V_{e_0}}\ = 0. \tag{A-12}$$

Here $m = \frac{\varphi}{2}$, s denotes Laplace variable and over bar – Laplace transform quantity.
The obtained solution of equation (A-10) and using (A-12) as,

$$\overline{U_{e_0}}\ = \frac{u_{e_0} \cos h\sqrt{m+\alpha+s}\ \chi}{s \cos h\sqrt{m+\alpha+s}}. \tag{A-13}$$

So, may utilize the complex inversion formula to invert Equation (A-13), therefore

$$\mathrm{y}\ (\tau)\ = \sum_n Res\ \ [\exp(s\tau)\ \overline{y}\ (s)]\ _{s=s_0}. \tag{A-14}$$

We can deduce from the theory of complex variables that R is the formula for the residue of a function G(z) at a simple pole at z = a.

$$\text{Res}\ \ [G(z)]_{z=a}\ = \lim_{z\to a}(z-a)G(z). \tag{A-15}$$

Hence to find the residue of equation (A-13)

$$\text{Res}\ \left[\frac{u_{e_0} \cos h\sqrt{m+\alpha+s}\ \chi}{s \cos h\sqrt{m+\alpha+s}}\ \right]$$

Hence, we get, simple pole at s = 0, there are infinitely many poles at s_n $=-(\pi^2(2n+1)^2+4m+4\alpha)$ where n = 0,1, 2...

$$U_{e_0}\ (\chi,\tau)\ \ = Res\ \ [s \cos h\sqrt{m+\alpha+s}]_{s=0} + Res\ \ [s \cos h\sqrt{m+\alpha+s}]_{s=s_n} \tag{A-16}$$

The first residue of equation (A-16)

$$Res\ \ [s \cos h\sqrt{m+\alpha+s}]_{s=0} = \lim_{s\to 0}\left[\frac{su_{e_0} \cos h\sqrt{m+\alpha+s}\ \chi\ exp(s\tau)}{s \cos h\sqrt{m+\alpha+s}}\right] = \frac{u_{e_0} \cos h\sqrt{m+\alpha}\ \chi}{\cos h\sqrt{m+\alpha}} \tag{A-17}$$

The second residue of equation (A-16)

$$Res\ \ [s \cos h\sqrt{m+\alpha+s}]_{s=s_n} = \lim_{s\to s_n}\left[\frac{u_{e_0} \cos h\sqrt{m+\alpha+s}\ \chi\ exp(s\tau)}{s \cos h\sqrt{m+\alpha+s}}\right] = \lim_{s\to s_n}\left[\frac{u_{e_0} \cos h\sqrt{m+\alpha+s}\ \chi\ exp(s\tau)}{s\frac{d}{ds}\cos h\sqrt{m+\alpha+s}}\right]$$

$$= -\ \frac{4\pi u_{e_0}\sum_{n=0}^{\infty}(-1)^n(2n\ +\ 1)\cos^{\pi}/_2(2n\ +\ 1)\chi e^{-\ \tau/_4(\pi^2(2n+1)^2+4m+4\alpha)}}{(\pi^2(2n+1)^2+4m+4\alpha)} \tag{A-18}$$

From equation (A-17) and (A-18) substitute in (A-16), we get

$$U_e(\chi,\tau) = \frac{u_{e_0} \cos h\sqrt{m+\alpha}\ \chi}{\cos h\sqrt{m+\alpha}}\ -\frac{4\pi u_{e_0}\sum_{n=0}^{\infty}(-1)^n(2n\ +\ 1)\cos^{\pi}/_2(2n\ +\ 1)\chi e^{-\ \tau/_4(\pi^2(2n+1)^2+4m+4\alpha)}}{(\pi^2(2n+1)^2+4m+4\alpha)}$$

Comparably, the text's (A-24) using Complex Inversion Formula, we can invert Equations (A-11).
The exact process is repeated in equations (A-18) and (A-19), giving us (A-25) and (A-26) in the text, respectively.

Appendix II: For the Limiting Case 1, the Degradation Concentration of Substrate α =0

In section 4, For enzyme and diffusion layers as follows,Using equations (A-28) for enzyme layer to construct new homotopy as follows,

$$(1-p)\left[\frac{\partial^2 U_e(\chi,\tau)}{\partial\chi^2}-\frac{\varphi^2 U_e(\chi,\tau)}{(1+U_e)_{((\chi=1)}}-\frac{\partial U_e(\ \chi,\tau)}{\partial\tau}\right]+p\left[\left(1+U_e(\chi,\tau)\right)\left(\frac{\partial^2 U_e(\chi,\tau)}{\partial\chi^2}\ -\frac{\partial U_e(\ \chi,\tau)}{\partial\tau}\right)-\varphi^2 U_e(\chi,\tau)\right]\ =\ 0 \tag{A-19}$$

$$(1-p)\left[\frac{\partial^2 U_e(\chi,\tau)}{\partial\chi^2}-\frac{\varphi^2 U_e(\chi,\tau)}{2}-\frac{\partial U_e(\ \chi,\tau)}{\partial\tau}\right]+p\left[\left(1+U_e(\chi\ \ \tau)\right)\left(\frac{\partial^2 U_e(\chi,\tau)}{\partial\chi^2}\ -\frac{\partial U_e(\ \chi,\tau)}{\partial\tau}\right)-\varphi^2 U_e(\chi,\tau)\right]\ =0 \tag{A-20}$$

Equating the coefficients of p

$$p^0\colon\ \frac{\partial^2 U_{e_0}\ (\chi,\tau)}{\partial\chi^2}-\frac{\varphi^2 U_{e_0}}{2}-\frac{\partial U_{e_0}\ (\ \chi,\tau)}{\partial\tau}\ =0 \tag{A-21}$$

The boundary conditions are:

$$\chi=0\ \ \frac{\partial U_{e_0}\ (\ \chi,\tau)}{\partial\chi}=0.$$

$$\chi=1\ \ U_{e_0}\ =u_{e_0}. \tag{A-22}$$

Taking Laplace transform in (A-20) to (A-22),

$$p^0\colon\ \frac{\partial^2\overline{U_{e_0}}}{\partial\chi^2}-m\overline{U_{e_0}}\ \ -s\overline{U_{e_0}}\ =0 \tag{A-23}$$

The boundary conditions become:

$$\chi=0\ \ \frac{\partial\overline{U_{e_0}}\ (\ 0)}{\partial\chi}=0,\chi=1\ \ \overline{U_{e_0}}\ \ =\frac{u_{e_0}}{s}. \tag{A-24}$$

Here m $=\frac{\varphi^2}{2}$, s denotes Laplace variable and over bar – Laplace transform quantity.
The obtained solution of equation (A-23) using (A-24) as,

$$\overline{U_{e_0}}\ \ =\frac{u_{e_0}\cos h\sqrt{m+s}\ \chi}{s\cos h\sqrt{m+s}}. \tag{A-25}$$

Then, following Appendix A process to get the solution of invert the enzyme substrate

$$U_e(\ \chi,\tau)\ =\ \frac{u_{e_0}\cos h\sqrt{m}\ \chi}{\cos h\sqrt{m}}-\frac{4\pi u_{e_0}\sum_{n=0}^{\infty}(-1)^n(2\mathrm{n}\ +\ 1)\cos{}^{\pi}/_{2}(2\mathrm{n}\ +\ 1)\chi e^{-\ \tau/_{4}(\pi^2(2n+1)^2+4m)}}{(\pi^2(2n+1)^2+4m)} \tag{A-26}$$

Similarly, the same processes of diffusion layer of substrate solution as,

$$U_d(\chi,\tau)\ =\frac{u_{d_1}\delta\ \sum_{n=0}^{\infty}(-1)^n(2\pi\mathrm{n})\sin(C\ -C(\chi))e^{-((C)^2)\tau}}{(C)^2}-\ \frac{u_{d_0}\delta\ \sum_{n=0}^{\infty}(-1)^n(2\pi\mathrm{n})\sin(C\ \chi-C(1+\delta))e^{-((C)^2)\tau}}{(C)^2}$$

Where C= $\frac{\mathrm{n}\pi}{\delta}$ & $m=\frac{\varphi^2}{2}$

Appendix III: For the Limiting Case 2, the Degradation Concentration of Product $\beta = 0$

In section 4, For enzyme and diffusion layers as follows, Using equations (A-16) for enzyme layer to construct new homotopy as follows,

$$(1-p)\left[\frac{\partial^2 V_e(\chi,\tau)}{\partial\chi^2}+\frac{\varphi^2 U_e(\chi,\tau)}{2}-\frac{\partial V_e(\ \chi,\tau)}{\partial\tau}\right]+p\left[\left(1+U_e(\chi,\tau)\right)\left(\frac{\partial^2 V_e(\chi,\tau)}{\partial\chi^2}\ -\frac{\partial V_e(\ \chi,\tau)}{\partial\tau}\right)+\varphi^2 U_e(\chi,\tau)\right]=\ 0 \tag{A-27}$$

Equating the coefficients of p

$$p^0\colon\ \frac{\partial^2 V_{e_0}\ (\chi,\tau)}{\partial\chi^2}+\frac{\varphi^2 U_{e_0}}{2}-\frac{\partial V_{e_0}\ (\ \chi,\tau)}{\partial\tau}\ =\ 0 \tag{A-28}$$

The boundary conditions:

$$\chi = 0 \;\; V_{e_0} = 0 \;\; \& \;\; \chi = 1 \;\; V_{e_0} = 0. \tag{A-29}$$

Taking Laplace transform in (A-28) to (A-29),

$$p^0: \; \frac{\partial^2 \overline{V_{e_0}}}{\partial \chi^2} + m\overline{U_{e_0}} - s\overline{V_{e_0}} = 0 \tag{A-30}$$

The boundary conditions become:

$$\chi = 0 \;\; \overline{V_{e_0}}(0) = 0 \;\; \& \;\; \chi = 1 \;\; \overline{V_{e_0}} = 0. \tag{A-31}$$

Here $m = \frac{\varphi^2}{2}$, s denotes Laplace variable and over bar – Laplace transform quantity.
The obtained solution of equation (A-30) and using (A-31) as,

$$\overline{V_{e_0}} = \frac{B\cos h\sqrt{s}\;\chi}{\cos h\sqrt{m+\alpha+s}(m)} + \frac{B\sin h\sqrt{s}\;\chi}{\sin h\sqrt{s}\;(m)} - \frac{B\sin h\sqrt{s}\;\chi\cos h\sqrt{s}}{\sin h\sqrt{s}\;(m)\cos h\sqrt{m+\alpha+s}} - \frac{B\cos h\sqrt{m+\alpha+s}\;\chi}{\cos h\sqrt{m+\alpha+s}(m)} \tag{A-32}$$

To convert in to complex inverse method to get the solution of enzyme layer product as,

$$V_e(\chi,\tau) = \frac{B}{\cos h\sqrt{m+\alpha}(m)} - \frac{4\pi B\sum_{n=0}^{\infty}(-1)^n(2n+1)\cos h\sqrt{\frac{(-A)}{4}}\;\chi e^{-\tau/4(A)}}{(A)(m)}$$

$$-\frac{B\cos h\sqrt{m+\alpha}\;\chi}{\cos h\sqrt{m+\alpha}(m)} + \frac{4\pi B\sum_{n=0}^{\infty}(-1)^n(2n+1)\cos(\frac{\pi}{2})(2n+1)\chi e^{-\tau/4(A)}}{(A)(m)} + \frac{4\pi B\sum_{n=0}^{\infty}(-1)^n(2n+1)\cos h\sqrt{\frac{(-A)}{4}}\;\sin h\sqrt{\frac{(-A)}{4}}\;\chi e^{-\tau/4(A)}}{(A)(m)\sin h\sqrt{\frac{(-A)}{4}}}$$

$$+\frac{B\sum_{n=0}^{\infty}(-1)^n(2\pi n)\sin n\pi\;\chi e^{-((\frac{n\pi}{\delta})^2+B)\tau}}{((n\pi)^2)(m)} - \frac{B\sum_{n=0}^{\infty}(-1)^n(2\pi n)\sin n\pi\;\chi e^{-((\frac{n\pi}{\delta})^2+\frac{B}{m})\tau}}{((n\pi)^2)(m)\cos h\sqrt{m-((n\pi)^2)}} \tag{A-33}$$

Where

$$\text{A}= \pi^2(2n+1)^2 + 4m + 4\alpha, \text{B} = mu_{e_0} \text{ and } = \frac{\varphi^2}{2}. \tag{A-34}$$

Similarly, the same processes of diffusion layer of product solution as,

$$V_d(\chi,\tau) = v_{d_0} - \frac{4\pi v_{d_0}\delta^2\sum_{n=0}^{\infty}(-1)^n(2n+1)\cos(\frac{\pi}{2(\delta)})(2n+1)(\chi-1-\delta)e^{-\frac{\tau(\pi^2(2n+1)^2)}{4\delta^2}}}{\pi^2(2n+1)^2} \tag{A-35}$$

Appendix IV: For the Limiting Case 3, the Degradation Concentration of Substrate and Product $\alpha = \beta = 0$

In section 4, For enzyme layer as follows, The equations in section 4 from (A-38) to (A-40) are solved by Akbari-Ganji method as follows,

$$\frac{\partial U_e(\chi,\tau)}{\partial \tau} = \frac{\partial^2 U_e(\chi,\tau)}{\partial \chi^2} - \frac{\varphi^2 U_e(\chi,\tau)}{1+U_e(\chi,\tau)} \tag{A-36}$$

$$\frac{\partial V_e(\chi,\tau)}{\partial \tau} = \frac{\partial^2 V_e(\chi,\tau)}{\partial \chi^2} + \frac{\varphi^2 U_e(\chi,\tau)}{1+U_e(\chi,\tau)} \;\; 0 < \chi < 1 \tag{A-37}$$

The initial and boundary conditions are:

$$\tau = 0, 0 < \chi < 1 \;\; U_e = 0, V_e = 0.$$

$$\chi = 0 \quad \frac{\partial U_e(\chi,\tau)}{\partial \chi} = 0, V_e = 0.$$

$$\chi = 1 \quad U_e = u_{e_0}, \quad V_e = 0.0 < \chi < 1 \tag{A-38}$$

Assume that solution of the equations (A-36) and (A-37)

$$U_e(\chi) = A_1 \cos h \ L_1\chi + B_1 \sinh L_1 \ \chi \tag{A-39}$$

$$V_e(\chi) = 1 + A_2 \cos h \ M_1\chi + B_2 \sinh M_1 \ \chi \tag{A-40}$$

Here A_1, B_1, A_2, B_2, L_1 and M_1 are constants has to be obtained.
To solve equation (A-39) using equation (A-38) to get

$$A_1 = \frac{u_{e_0}}{\cos hL_1} \ , \ B_1 = 0 \tag{A-41}$$

From equation (A-41) substitute in equation (A-39)

$$U_e(\chi) = \frac{u_{e_0}}{\cos hL_1} \cos h \ L_1\chi \tag{A-42}$$

Substitute equation (A-42) in to (A-36) we get,

$$\left(1 + \frac{u_{e_0}}{\cos hL_1} \cos h \ L_1\chi \right) {L_1}^2 \frac{u_{e_0}}{\cos hL_1} \cos h \ L_1\chi \ - \varphi^2 \ \frac{u_{e_0}}{\cos hL_1} \cos h \ L_1\chi \ = 0 \tag{A-43}$$

Put $\chi = 1$ in equation (A-43),

$$L_1 = \frac{\varphi}{\sqrt{1+u_{e_0}}}$$

By repeating the same procedure in equation (A-40) using equation (A-38), we get in the text.

Appendix V: MATLAB (pdex4) Numerical Solution

```
function pdex4
m = 0;
x = linspace(0,1);
t = linspace(0,0.25);
sol = pdepe(m,@pdex4pde,@pdex4ic,@pdex4bc,x,t);
u1 = sol(:,:,1);
u2 = sol(:,:,2);
%---------------------------------------------------------------------
%figure
%plot(x,u1(end,:))
%title( 'u1(x)')
%xlabel( 'Dimensionless Distance x')
%ylabel( 'Dimensionless concentration u')
%---------------------------------------------------------------------
figure
plot(x,u2(end,:))
title( 'u2(x)')
xlabel( 'Dimensionless Distance x')
ylabel( 'Dimensionless concentration v')
% ---------------------------------------------------------------------
function [c,f,s] = pdex4pde(x,t,u,DuDx)
c = [1; 1];
```

```
f = [1; 1].*DuDx;
m= 3;
a= 2;
b= 2;
F1 =-a*u(1)-(m*u(1))/(1+u(1));
F2 =-b*u(2)+(m*u(1))/(1+u(1));
s = [F1; F2;];
function u0 = pdex4ic(x) %create a initial conditions
u0 = [0; 0];
% ---------------------------------------------------------------
function [pl,ql,pr,qr]= pdex4bc(xl,ul,xr,ur,t) %create a boundary conditions
pl = [0; ul(2)];
ql = [1; 0];
pr = [ur(1)-1; ur(2)];
qr = [0; 0];
```

References

[1] Turner A. P. F, Karube I, Wilson G. S (eds.), "Biosensors: Fundamentals and Applications" (Oxford University Press, Oxford, 1987.

[2] Fraser D. M. (ed.), Biosensors in the Body: Continuous in vivo Monitoring. Wiley Series in Biomaterials Science and Engineering (Wiley, New York, 1997).

[3] Baronas R, Ivanauskas F, and Kulys J, "Computational modelling of the behaviour of Potentiometric membrane biosensors," J. Math. Chem., vol. 42, pp. 321–336, 2007.

[4] Baronas R, Ivanauskas F, and Kulys J, Mathematical Modeling of Biosensors: An Introduction for Chemists and Mathematicians, Springer Series on Chemical Sensors and Biosensors, vol. 9 (Springer, Berlin, 2010).

[5] Baronas R, Ivanauskas F, and Kulys J, and Sapagovas M, "Modelling of amperometric biosensors with rough surface of the enzyme membrane," J. Math. Chem., vol. 34, pp. 227–242, 2003.

[6] Baronas R, Kulys J and Ivanauskas F "Modelling amperometric enzyme electrode with substrate cyclic conversion," Biosens. Bioelectron., vol. 19, pp. 915–922, 2004.

[7] Stikoniene O, Ivanauskas F, Laurinavicius V. "The influence ˙ of external factors on the operational stability of the biosensor response," Talanta 81, 1245 (2010).

[8] Meskauskas, F. Ivanauskas, and Laurinavicius V. "Degradation ˇ of substrate and/or product: mathematical modeling of biosensor action," J. Math. Chem., 2013, accepted for publication, https://doi.org/10.1007/s10910-013-0223-y

[9] Meskauskas T, Ivanauskas F and Laurinavicius V. "Numerical Modeling of Multilayer Biosensor with Degrading Substrate and Product" © 2013 IEEE. https://doi.org/10.1109/EUROSIM.2013.15

[10] Sengupta, J., & Hussain, C. M. (2025). MXene-Based Electrochemical Biosensors: Advancing Detection Strategies for Biosensing (2020–2024). *Biosensors*, *15*(3), 127.

[11] Shafie, A., & Adnan Ashour, A. (2025). Advances in Organic Fluorescent and Colorimetric Probes for The Detection of Cu^{2+} and Their Applications in Cancer Cell Imaging (2020–2024). *Critical Reviews in Analytical Chemistry*, 1-27.

[12] Swaminathan R, Chithra Devi M, Rajendran L, Venugopal K. Sensitivity and resistance of Amperometric Biosensor in substrate inhibition, *J. Electroanal. Chem.* 2021; 895: 115527.

[13] Al-Ahmary, K. M., Shafie, A., Adnan Ashour, A., S. Alrashdi, K., Babalghith, A. O., Alharthi, S. S., & Sabei, F. Y. (2024). Recent Advances in Calixarenes for the Detection of Metal Ions, Bioimaging Applications, and Anticancer Activities: A Comprehensive Review (2020–2024). *Critical Reviews in Analytical Chemistry*, 1-26.

[14] Drobysh, M. (2024). *Electrochemical biosensors for COVID-19 diagnosis* (Doctoral dissertation, Vilniaus universitetas).

[15] Preethi KPV, Chitra Devi M, Swaminathan R, Poovazhaki R. The New Homotopy Perturbation Method (NHPM) for nonlinear parabolic Equation in chemical sciences *International Journal of Mathematics and its applications*, 2018; 6: 359-367.

[16] Ashour, A. A., & Shafie, A. (2024). Recent progress in cellulose derivatives and cellulose-based composites for bioimaging and anticancer applications (2020–2024). *Cellulose*, 1-24.

[17] Ranjani K, Vijayalakshmi L. Choquet Integral Compared With Weighted Mean In Decision Making, *IJMTT* 2020.

[18] Ranjani K, Swaminathan R, Karpagavalli SG. Mathematical modelling of a mono-enzyme dual amperometric biosensor for enzyme-catalyzed reactions using homotopy analysis and Akbari-Ganji methods, *Int. J. Electrochem. Sci*, 2023; 18(9): 100220.

[19] Reena A, Karpagavalli SG, Rajendran L, Manimegalai B, Swaminathan R. Theoretical analysis of putrescine enzymatic biosensor with optical oxygen transducer in sensitive layer using Akbari- Ganji method" Int. J. Electrochem. Sci 2023; 18(5): 100113.

[20] Nebiyal A, Swaminathan R, Karpagavalli SG. Reaction kinetics of amperometric enzyme electrode in various geometries using the Akbari-Ganji methods. *Int. J. Electrochem. Sci* 2023; 18(9): 100240.

[21] Raju, R. V., Karpagavalli, S. G., & Swaminathan, R. (2024). Nonlinear Steady-State VOC and Oxygen Modeling in Biofiltration. *International Journal of Analysis and Applications*, *22*, 155.

[22] Ranjani K, Swaminathan R, Karpagavalli SG. A theoretical investigation of steady-state concentration processes at a carrier-mediated transport model using Akbari-Ganji and differential transform methods" *Partial Differ. Equ. Appl.*, 2023: 8: 100594.

[23] Uma, A., Raja, R., & Swaminathan, R. (2024). Analytical Solution of Concentrated Mixtures of Hydrogen Sulfide and Methanol in Steady State in Biofilm Model. *Contemporary Mathematics*, 2632-2645.

[24] Uma, A., & Swaminathan, R. (2024). Mathematical Analysis of Nonlinear Reaction Diffusion Process at Carbon Dioxide Absorption in Concentrated Mixtures of 2-Amino-2-Methyl-1-Proponal and 1, 8-Diamino-p-Methane. *International Journal of Analysis and Applications*, *22*, 110.

[25] Nebiyal, A., Swaminathan, R., Raja, R., & Karpagavalli, S. G. (2024). Investigation of a Mathematical Model and Non-Linear Effects Based on Parallel-Substrates Biochemical Conversion. *Contemporary Mathematics*, 2198-2210.

[26] Manimegalai, B., Rajendran, L., & Lyons, M. E. G. (2021). Theory of the transient current response for the homogeneous mediated enzyme catalytic mechanism at the rotating disc electrode. *International Journal of Electrochemical Science*, *16*(9), 210946.

[27] Ranjani, K., Swaminathan, R., & Karpagavalli, S. G. (2024, August). A study on analytical non-linear theory of the porous fin in heat transfer using Akbari-Ganji method. In *AIP Conference Proceedings* (Vol. 3160, No. 1). AIP Publishing.

[28] Kirthiga, O. M., & Rajendran, L. (2015). Approximate analytical solution for non-linear reaction diffusion equations in a mono-enzymatic biosensor involving Michaelis–Menten kinetics. *Journal of Electroanalytical Chemistry*, *751*, 119-127.

[29] Ranjani, K., Swaminathan, R., & Karpagavalli, S. G. (2024). Mathematical modelling of three-layer amperometric biosensor and analytical expressions using homotopy perturbation method. *Partial Differential Equations in Applied Mathematics*, 100755.

[30] Nebiyal, A., Swaminathan, R., & Karpagavalli, S. G. (2024). Mathematical Modelling and Application of Analytical Methods for A Non-Linear EC2E Mechanism in Rotating Disk Electrode. *International Journal of Analysis and Applications*, *22*, 92.